

# Magnetic dichroism in angular resolved XPS on the Fe(110) surface

Yu.S. Dedkov<sup>a</sup>

Institut für Festkörperphysik, Technische Universität Dresden, 01062 Dresden, Germany

Received 8 June 2005 / Received in final form 26 July 2005

Published online 11 October 2005 – © EDP Sciences, Società Italiana di Fisica, Springer-Verlag 2005

**Abstract.** Magnetic dichroism has been observed in the angular distribution of Fe  $2p$  photoemission spectra from Fe(110) surface by unpolarized Al  $K\alpha$  X-rays. The dichroism asymmetry varies strongly around low-index forward-scattering direction in the Fe thin film. Photoelectron diffraction theory provides explanation for these unpolarized dichroism effects, which should also be generally useful in surface magnetism studies.

**PACS.** 75.70.-i Magnetic properties of thin films, surfaces, and interfaces – 61.14.Qp X-ray photoelectron diffraction

## 1 Introduction

Magnetic dichroism in core-level photoemission from solids represents a promising new element-specific probe to investigate the magnetic structure of surfaces and interfaces. One way to measure such effects is to use photoelectrons excited by circularly polarized light, for which even the spin-integrated intensity depends on the relative orientation of the photon helicity (left or right circularly polarized) and the sample magnetization (X-ray magnetic circular dichroism in photoemission, XMCD in PE). Purely atomic models have been successfully applied to explain many aspects of such data [1–3]. Another example of dichroism experiment is using the  $p$ -type linearly polarized light with an electric-field component perpendicular to the surface (X-ray magnetic linear dichroism, XMLD) [4]. Intensive experimental and theoretical investigations of XMLD and diffraction effects in it were carried out on Fe(100) surface as well as on Co/Fe(100) interface in the recent works [5–8]. It has been previously shown that magnetic dichroism from core levels can be also observed with unpolarized light [9–13]. The fact that the photoelectron intensity with unpolarized radiation ( $I_{unp}$ ) can be simply related to those with both  $s$  and  $p$  linear, and right and left circular polarization via  $I_{unp} = I_s + I_p = I_{RCP} + I_{LCP}$  also makes clear the close connection among them. Thus off-normal unpolarized light contains the  $p$  component producing XMLD, and X-ray magnetic dichroism with unpolarized radiation (XMUD) can be viewed as a special manifestation of XMLD.

XMCD in PE was immediately explained in terms of the selection rules for dipole-allowed transitions from

*initial states* that are split by both spin-orbit and exchange effects, with the latter being directly related to the magnetization of the sample [14,15]. The potential importance of photoelectron diffraction effects in the *final states* of the excitation have also been pointed out and such effects have been shown to play a role in XMLD and XMUD [10,11,16]. However, a complete understanding of XMLD and XMUD including both initial-state and final-state effects is yet to be obtained. In the present investigation, we explore magnetic dichroism occurring with unpolarized light in different experimental geometry for the Fe(110) surface, and compare present results with other measurements on another crystallographic planes of iron. We find that a model including both initial- and final-state effects is essential for interpretation.

## 2 Experimental details

The experimental geometry is shown schematically in Figure 1. Al  $K\alpha$  radiation impinges on the sample in the  $x-z$  plane at an angle  $60^\circ$  with respect to the photoelectron collection direction. The sample magnetization is switched by magnetic field of about 500 Oe between the  $+y$  and  $-y$  directions to obtain the dichroism. The sample can be rotated about the  $y$  axis to vary the angle  $\alpha$ , which equals to zero for the emission normal to the surface. In this case only emission direction with respect to the crystal lattice was varied, while keeping the geometrical conditions between  $\mathbf{M}$  (magnetization),  $\mathbf{k}$  (photoelectron wave vector), and  $\mathbf{E}$  (electric field vector) constant. We used a standard X-ray source emitting unpolarized Al  $K\alpha$  radiation and CLAM energy analyzer accepting electrons over a cone with about a  $5^\circ$  full acceptance angle. The overall energy resolution was 0.9 eV as obtained from the width of

<sup>a</sup> e-mail: dedkov@physik.phy.tu-dresden.de

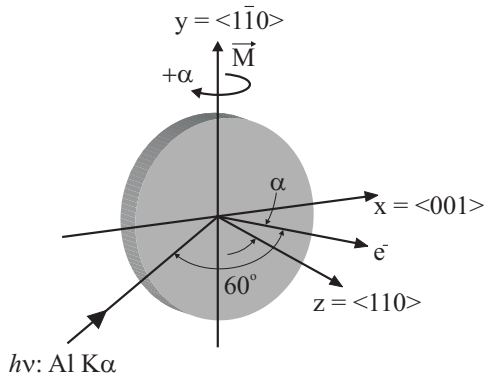


**Fig. 1.** The photoemission geometry of the dichroism experiment on Fe(110) surface.

the Ag Fermi edge. The samples were 30 Å thick epitaxial Fe(110) films grown *in situ* on W(110) substrate in UHV conditions with an in-plane easy magnetization direction ( $y = \langle 1\bar{1}0 \rangle$ ) coinciding with the axis of rotation. The cleanliness and crystallographic order of the substrate and the Fe films were checked by XPS and low energy electron diffraction (LEED).

### 3 Results and discussion

Figures 2a and 2b show the crystallographic structure of the Fe(110) surface from the top and side view, respectively. The black rectangular means the unit cell of the Fe(110) surface with crystallographic parameters of 2.87 Å along  $\langle 001 \rangle$  direction and 4.05 Å along  $\langle 1\bar{1}0 \rangle$  direction. The corresponding LEED patterns obtained at energy of primary electron beam of 110 eV are presented as an inset in Figure 2a.

Figure 3 shows (a) Fe  $2p$  as well as  $3p$  XPS spectra at normal emission and (b) intensity variation of the  $2p_{3/2}$ ,  $2p_{1/2}$  and  $3p$  photoelectron peaks in dependence on emission angle  $\alpha$ . The intensity variation curves displays the photoelectron diffraction peaks occurring at emission angles of  $\alpha = 0^\circ$ ,  $16.5^\circ$ , and  $33^\circ$  that are due to the strong forward scattering along the  $\langle 110 \rangle$ ,  $\langle 221 \rangle$ , and  $\langle 111 \rangle$  directions, and which should ideally occur at  $\alpha = 0^\circ$ ,  $19.4^\circ$ , and  $35.3^\circ$ . These directions are shown in Figure 2b by black arrows.

The XPS spectra of the Fe(110) films recorded for opposite magnetization directions reveal a small but distinct difference in both peak intensity and energy position (not shown here). The apparent shift between  $M = \uparrow$  and  $M = \downarrow$  spectrum is of opposite sign for the  $2p_{3/2}$  and  $2p_{1/2}$  lines. This gives rise to the characteristic dichroic signal which is presented in Figure 4a, with a plus/minus feature at  $2p_{3/2}$  and a minus/plus feature at  $2p_{1/2}$ . We refer to the dichroic signal as an intensity asymmetry  $A(E)$ , i.e., the difference of the intensity spectra taken at opposite magnetization directions divided by their sum. The shape of the asymmetry spectrum resembles closely those observed earlier for the Fe(100) surface [10, 11, 17]. Figure 4b shows

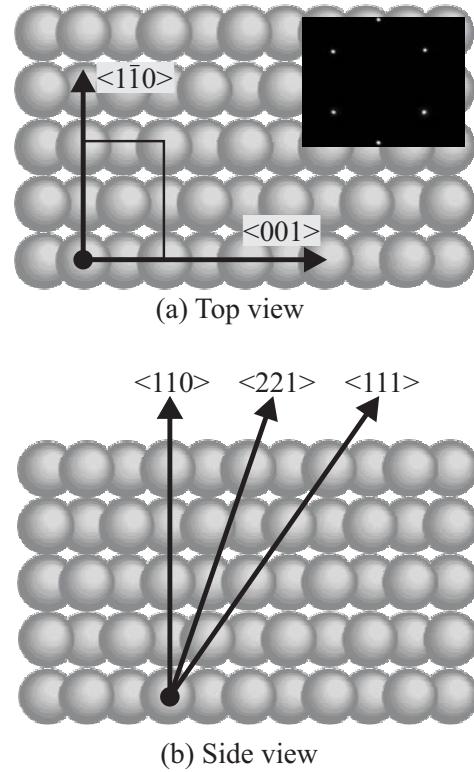


**Fig. 2.** Crystallographic structure of the (110) surface of iron: (a) top view, (b) side view. Inset of (a) shows corresponding LEED pattern of Fe(110) surface obtained at an energy of 110 eV of primary electron beam.

the gray-scale contour map of the angular resolved XMUD asymmetry in the region of Fe  $2p_{3/2}$  photoemission peak. The line profile around  $\alpha = 0^\circ$  and kinetic energy of about 782.5 eV shown as an inset in Figure 4a. The maximum of the dichroism asymmetry occurs at an emission angles of  $\alpha = -10^\circ$ ,  $+1^\circ$ , and  $+11^\circ$  and the minimum at  $\alpha = -5^\circ$  and  $+7^\circ$ .

In works [10, 11] the magnetic dichroism has been measured in angle-resolved core-level photoemission from the Fe  $2p$  and  $3p$  levels from Fe(100) epitaxial films. The intensity of peaks also shown diffraction patterns that are dominated by forward scattering along low-index crystallographic directions. As it was observed, the dichroism signal along these emission angles was very small and exhibited sign changes around each of them as  $\alpha$  was varied. This effect leads in works [10, 11] to a characteristic “chess-board” patterns that are nearly centered in  $(\alpha, E_{kin})$  along the forward scattering peaks. In the present work this effect is absent and dichroism asymmetry is always positive at kinetic energy of 782.5 eV. But intensity of the dichroic signal strongly depends on the emission angle with respect to low-index directions in the crystal lattice. This fact immediately indicate that photoelectron diffraction is a primary factor which influences on the dichroic asymmetry signal since the relations between  $\mathbf{M}$ ,  $\mathbf{k}$ , and  $\mathbf{E}$  which in a single-atom picture [18] exclusively determine the dichroism are not affected by the rotation in the present experiment. The simple and heuristic model

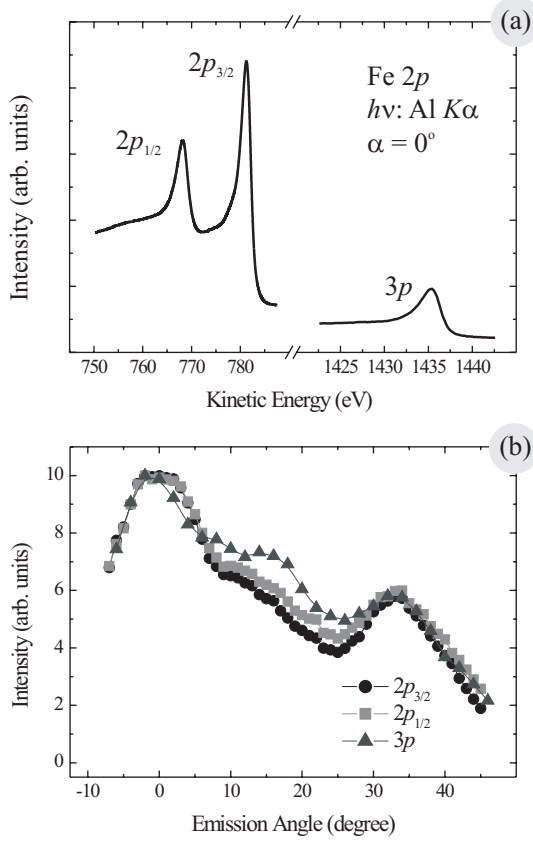


**Fig. 3.** (a) Fe  $2p$  and  $3p$  photoemission spectra for 30 Å thick epitaxial Fe film on W(110) substrate (emission angle  $\alpha = 0^\circ$ ). (b) Intensity variation of the  $2p_{3/2}$ ,  $2p_{1/2}$  and  $3p$  photoemission peaks in dependence on emission angle  $\alpha$ .

of the diffraction effect in dichroism is following. The left-right asymmetric dichroism pattern was shown to arise because the intensity differences of the  $\pm m_j$  pairs (whose energy positions are simply interchanged by switching the magnetization direction) and given by the following formula [10,11]:

$$I\left(\frac{3}{2}, m_j\right) - I\left(\frac{3}{2}, -m_j\right) \propto (|f(\alpha)|/R) \sin[\delta(\alpha)] \times (1 - \cos 2\alpha - 3 \sin 2\alpha), \quad (1)$$

where  $\alpha$  is the emission angle with respect to the emitter-scatterer bond axis,  $|f(\alpha)|$  is the magnitude of the scattering factor,  $R$  is the distance between emitter and scatterer, and  $\delta(\alpha)$  is the total phase difference between direct and scattered waves due to both scattering and path length difference. This formula was applied to the diatomic case of a single emitter and a single scatterer in work [10] for the case of Fe(100) surface, and it makes it clear that a left-right asymmetry due to electron scattering and diffraction will arise as  $\alpha$  passes from the negative  $\alpha$  to the positive ones around emitter-scatterer direction ( $\alpha = 0^\circ$ ). This qualitative explanation together with more detailed theory were successfully applied to explain diffraction effect in dichroism on the Fe(100) surface [10,11].

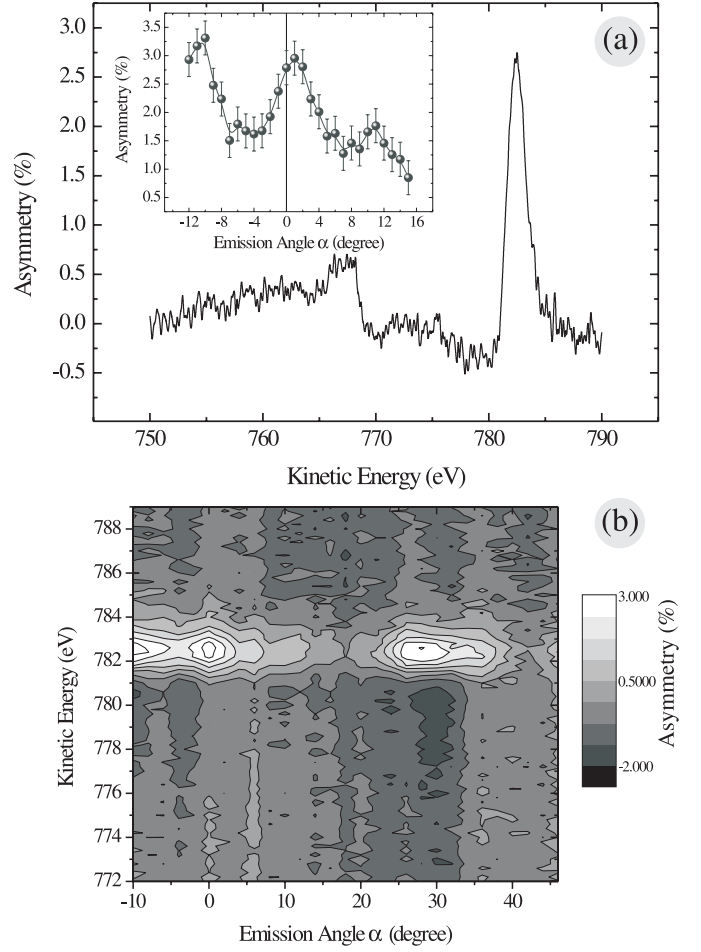


**Fig. 4.** (a) Dichroic intensity asymmetry  $A(E)$  measured at emission angle  $\alpha = 0^\circ$ . (b) Gray-scale contour map of the angular resolved XMUD asymmetry [line profile around  $\alpha = 0^\circ$  and kinetic energy of 782.5 eV shown as inset in (a)].

It is clear from (1) that in free atom-like case at small  $\alpha$  around forward scattering at  $0^\circ$  the dichroism asymmetry is proportional to  $\alpha$ , i.e. antisymmetric and it has to change a sign. In our case of Fe(110) thin film the dichroism assembly also shows the antisymmetric behavior but always positive. This is surely a deviation from the atomic description of the dichroism. This deviation from the atomic description and from the results of previous works must be attributed to the crystallinity of the sample, which is not included in atomic models as well as to the lower symmetry of the *bcc* Fe(110) surface compare to the *bcc* Fe(100) [10,11] and *fcc* Co(100) [19] surfaces. Besides, the crystallinity of the sample may manifest itself also in effects not related to photoelectron scattering. The atomic model is valid only for an isolated atom that is polarized along  $\mathbf{M}$ , but has an otherwise spherically symmetric electronic configuration. This is surely not a valid description for atoms in solid. There the atoms and their electronic orbitals are kept fixed in space. In addition, a directional redistribution of the electronic states compared to free atoms due to the presence of neighboring atoms may occur. In such a case the photoelectron will probe

a non-spherical potential, and as a consequence the outgoing electron wave (direct wave) could present a small angular dependence [20].

## 4 Conclusion

In conclusion we reported an observation of angular-resolved XMUD effect on the thin epitaxial Fe(110) films grown on W(110) substrate, using unpolarized Al  $K\alpha$  radiation. In the presented experimental geometry a strong deviation from the angular behavior of the dichroic asymmetry expected within an atomic description as well as from the previous experimentally observed angular dependence of the asymmetry on the Fe(100) and Co(100) surfaces is shown. That deviation is related to crystallinity effects, which are found to be mainly governed by diffraction from forward scattering and lowest symmetry of the Fe(110) surface compare to *bcc* and *fcc* (100) surface used in previous experiments.

## References

1. N.A. Cherepkov, Phys. Rev. B **50**, 13813 (1994)
2. D. Venus, Phys. Rev. B **49**, 8821 (1994)
3. G. van der Laan, E. Arenholz, E. Navas, A. Bauer, G. Kaindl, Phys. Rev. B **53**, R5998 (1996)
4. Ch. Roth, F.U. Hillebrecht, H.B. Rose, E. Kisker, Phys. Rev. Lett. **70**, 3479 (1993)
5. G. Rossi, G. Panaccione, F. Sirotti, N.A. Cherepkov, Phys. Rev. B **55**, 11483 (1997)
6. G. Rossi, G. Panaccione, F. Sirotti, S. Lizzit, A. Baraldi, G. Paolucci, Phys. Rev. B **55**, 11488 (1997)
7. G. Panaccione, F. Sirotti, G. Rossi, Solid State Commun. **113**, 373 (2000)
8. F. Bruno, G. Panaccione, A. Verdini, R. Gotter, L. Floreano, P. Torelli, M. Sacchi, F. Sirotti, A. Morgante, G. Rossi, Phys. Rev. B **66**, 024417 (2002)
9. M. Getzlaff, Ch. Ostertag, G.H. Fecher, N.A. Cherepkov, G. Schönhense, Phys. Rev. Lett. **73**, 3030 (1994)
10. A. Fanelisa, R. Schellenberg, F.U. Hillebrecht, E. Kisker, J.G. Menchero, A.P. Kaduwela, C.S. Fadley, M.A. Van Hove, Phys. Rev. B **54**, 17962 (1996)
11. R. Schellenberg, E. Kisker, A. Fanelisa, F.U. Hillebrecht, J.G. Menchero, A.P. Kaduwela, C.S. Fadley, M.A. Van Hove, Phys. Rev. B **57**, 14310 (1998)
12. G. Panaccione, F. Sirotti, S. Lizzit, A. Baraldi, G. Paolucci, N.A. Cherepkov, G. Rossi, Surf. Sci. **377–379**, 440 (1997)
13. J. Morais, G.H. Fecher, R. Denecke, J. Liesegang, C.S. Fadley, J. Elec. Spec. Rel. Phen. **114–116**, 783 (2001)
14. L. Baumgarten, C.M. Schneider, H. Petersen, F. Schäfers, J. Kirschner, Phys. Rev. Lett. **65**, 492 (1990)
15. D. Venus, L. Baumgarten, C.M. Schneider, C. Boeglin, J. Kirschner, J. Phys.: Condens. Matter **5**, 1239 (1993)
16. F.U. Hillebrecht, H.B. Rose, T. Kinoshita, Y.U. Idzerda, G. van der Laan, R. Denecke, L. Ley, Phys. Rev. Lett. **75**, 2883 (1995)
17. C.M. Schneider, U. Pracht, W. Kuch, A. Chassé, J. Kirschner, Phys. Rev. B **54**, R15618 (1996)
18. N.A. Cherepkov, V.V. Kuznetsov, V.A. Verbitskii, J. Phys. B: At. Mol. Opt. Phys. **28**, 1221 (1995)
19. X. Gao, M. Salviatti, W. Kuch, C.M. Schneider, J. Kirschner, J. Electron Spectrosc. Relat. Phenom. **113**, 137 (2001)
20. P. Rennert, Yu. Kucherenko, J. Electron Spectrosc. Relat. Phenom. **76**, 157 (1995)